Title

Divergent Mechanisms Leading to Signaling Dysfunction in Embryonic Muscle by Bisphenol A and Tetrabromobisphenol A

Journal

Molecular Pharmacology, 91(4)

ISSN

0026-895X

Authors

Zhang, Rui
Pessah, Isaac N

Publication Date

2017-04-01

DOI

10.1124/mol.116.107342

Peer reviewed

1521-0111/91/4/428–436$25.00
MOLECULAR PHARMACOLOGY

http://dx.doi.org/10.1124/mol.116.107342
Mol Pharmacol 91:428–436, April 2017

Divergent Mechanisms Leading to Signaling Dysfunction in Embryonic Muscle by Bisphenol A and Tetrabromobisphenol A

Rui Zhang and Isaac N. Pessah

Department of Molecular Biosciences, School of Veterinary Medicine, University of California Davis, Davis (R.Z., I.N.P.), and The Medical Investigation of Neurodevelopmental Disorders (MIND) Institute, Sacramento (I.N.P.), California

Received November 4, 2016; accepted January 26, 2017

ABSTRACT

Bisphenol A (BPA) and its brominated derivative tetrabromobisphenol A (TBBPA) are high production volume chemicals used in the manufacture of various consumer products. Although regarded as endocrine disruptors, these chemicals are suspected to exert nongenomic actions on muscle function that are not well understood. Using skeletal muscle microsomes, we examined the effects of BPA and TBBPA on ryanodine receptor type 1 (RyR1), dihydropyridine receptor (DHPR), and sarcoplasmic/endoplasmic reticulum Ca^{2+} ATPase (SERCA). We assessed the impact of these chemicals on Ca^{2+} dynamics and signaling in embryonic skeletal myotubes through fluorescent Ca^{2+} imaging and measurement of resting membrane potential (V_m). TBBPA activated RyR1 and inhibited DHPR and SERCA, inducing a net efflux of Ca^{2+} from loaded microsomes, whereas BPA exhibited little or no activity at these targets. Regardless, both compounds disrupted the function of intact myotubes. TBBPA diminished and eventually abrogated Ca^{2+} transients, altered intracellular Ca^{2+} equilibrium, and caused V_m depolarization. For some cells, BPA caused rapid Ca^{2+} transient loss without marked changes in cytosolic and sarcoplasmic reticulum Ca^{2+} levels, likely owing to altered cellular excitability as a result of BPA-induced V_m hyperpolarization. BPA and TBBPA both interfere with skeletal muscle function through divergent mechanisms that impair excitation-contraction coupling and may be exemplary of their adverse outcomes in other muscle types.

Introduction

Bisphenol A (BPA) and its brominated derivative tetrabromobisphenol A (TBBPA) are both high production volume chemicals whose consumption has increased in recent decades owing to their ubiquitous inclusion into various consumer products. BPA is a necessary component in producing polycarbonate plastic and epoxy resins, and its annual worldwide production exceeds 2.5 million metric tons (Vandenberg et al., 2007). TBBPA, in comparison, is used primarily as a brominated flame retardant in electrical and electronic equipment, with annual global demand for this chemical exceeding 120,000 metric tons (Birnbaum and Staskal, 2004). With the inclusion of BPA into a variety of common goods (e.g., water bottles, sports equipment, medical devices, food and beverage can lining, thermal paper) and TBBPA into a large range of devices (e.g., televisions, cell phones, computers), these two chemicals have achieved a certain universality and wide reach that impacts populations worldwide. As such, both BPA and TBBPA are routinely detected in both human tissue and environmental samples (Kang et al., 2006; vom Saal et al., 2007; Johnson-Restrepo et al., 2008; Vandenberg et al., 2010) and are indeed considered universal environmental pollutants. Numerous studies prompted by these concerns have examined the toxicologic effects of BPA and TBBPA; despite the current state of the science, more mechanistic research is needed to understand the potential impacts of these and similarly structured chemicals on human health.

Of all the findings regarding BPA and TBBPA, the most salient concern regarding these chemicals is their ability to disrupt endocrine signaling (Vandenberg et al., 2009; Shaw et al., 2010). BPA has perhaps garnered the most attention of all endocrine-disrupting chemicals in the scientific and lay communities. BPA is weakly estrogenic, and TBBPA structurally mimics the thyroid hormone thyroxine, yet evidence indicates that the actions of both chemicals are not limited to the perturbation of the endocrine system through their respective hormone receptors (Westerink, 2014; Soriano et al., 2016). Recent studies have shown that BPA is capable of interacting with various ionic currents, and TBBPA can alter Ca^{2+} fluxes and homeostasis in cellular systems. Intracellular ionized Ca^{2+} is a universal second messenger associated with myriad signaling processes that govern cell function, and BPA and TBBPA's ability to alter Ca^{2+} signaling presents a mode of

This work was sponsored by the National Institutes of Health (NIH) National Institute of Environmental Health Sciences [Grants P01 ES011269, R01 ES014901, and R01 ES020392], National Institute of Arthritis and Musculoskeletal and Skin Diseases [Grant P01 AR052354], and Intellectual and Developmental Disabilities Research Center core grant [Grant U54 HD079125] to I.N.P.; NIH training fellowships [Grants T32 ES007059 and T32 HL086350] to R.Z.
dx.doi.org/10.1124/mol.116.107342.

ABBREVIATIONS: ANOVA, analysis of variance; AP-III, antipyrylazo-III; BPA, bisphenol A; Caff, caffeine; DHPR, dihydropyridine receptor; DMSO, dimethyl sulfoxide; ECC, excitation-contraction coupling; F, fluorescence (arbitrary units); F_0, baseline fluorescence; F_{max}, maximal fluorescence (peak); PCB, polychlorinated biphenyl; ppb, parts per billion; RyR1, type 1 ryanodine receptor (skeletal muscle isoform); SERCA, sarcoplasmic/endoplasmic reticulum Ca^{2+} ATPase; SR, sarcoplasmic reticulum; TBBPA, tetrabromobisphenol A; TCS, triclosan; V_m, membrane potential.

toxicologic action that could extend to numerous physiologic systems, including endocrine pathways. Indeed, studies have emerged that designate BPA as a cardiotoxicant for its capacity to promote cardiac arrhythmias in isolated hearts and cardiomyocytes (Yan et al., 2011; Posnack et al., 2014); likewise, TBBPA has been implicated as a neurotoxicant for its Ca^{2+} dysregulation in neuronal cells (Reistad et al., 2007; Hendriks et al., 2012). These studies provided a basis for us to investigate the molecular targets of Ca^{2+} dysregulation of BPA and TBBPA in a well understood Ca^{2+} signaling system, skeletal muscle excitation-contraction coupling (ECC), which has yet to be examined with these chemicals.

In skeletal muscle, Ca^{2+} plays a critical role in muscular contraction initiated by a process termed *ECC* that conveys electrical stimuli (action potentials) on the myocyte surface (sarcolemma) to release internal Ca^{2+} stored in the sarcoplasmic reticulum (SR). Two proteins essential for ECC in skeletal muscle are the dihydropyridine receptor (DHPR; L-type Ca^{2+} channel) within the sarcolemma and the type 1 ryanodine receptor (RyR1) within the SR. A third key protein is the sarcoplasmic/endoplasmic reticulum Ca^{2+} ATPase (SERCA) that mediates relaxation by actively pumping intracellular Ca^{2+} back into the SR.

As an intricate Ca^{2+}-mediated process involving the interplay of several critical proteins, ECC may be dysregulated through diverse means, including several mutations as well as environmental pollutants of concern to human health, including non-dioxin-like polychlorinated biphenyls (PCBs), brominated flame retardants, and triclosan (TCS) (Pessah et al., 2010). Since both BPA and TBBPA share similar chemical properties with RyR-active chemicals, we postulated that differences in bromination between the two compounds could differentially influence the activities of RyR1, as well as DHPR and SERCA, resulting in distinguishable impairments in ECC in an embryonic form of primary skeletal muscle (myotubes) isolated from neonatal mice. Here, we show that BPA and TBBPA can impair myotube ECC, which can be ascribed to their divergent interactions with DHPR, RyR1, and SERCA, identifying direct mechanisms that impair muscle Ca^{2+} regulation and function.

Materials and Methods

Chemicals. Bisphenol A (BPA, ≥99%, CAS no. 80-05-7) and tetrabromobisphenol A (TBBPA, 97%, CAS no. 79-94-7) were obtained from Sigma-Aldrich (St. Louis, MO) (structures shown in Fig. 7). Triclosan (TCS, ≥97%, CAS Number 3380-34-5) was obtained from Sigma-Aldrich as Irgasan. Stock solutions were made by dissolving test chemicals in dimethyl sulfoxide (DMSO); final DMSO concentrations for experiments did not exceed 0.1% in buffer unless otherwise stated. [^{3}H]Ryanodine (95.0 Ci/mmol) and [^{3}H]PN200 (83.7 Ci/mmol) were obtained from PerkinElmer Life and Analytical Sciences (Waltham, MA).

Animals. All collection of mouse and rabbit tissues was conducted under protocols approved by the Institutional Animal Care and Use Committee (IACUC) at the University of California, Davis.

Preparation of Total Membrane Fractions. Skeletal muscles were collected from the hind legs and back of wild-type male New Zealand White rabbits weighing 3–5 kg, obtained from Charles River (Burlington, MA). The muscles were stored at -80°C until processed. We ground 75 g of tissue using a meat grinder and subsequently homogenized this tissue in 10 volumes of ice-cold buffer (10% sucrose, 10 mM HEPES, 10 μg/ml leupeptin hydrochloride, 100 μM phenylmethanesulfonylfluoride, pH 7.4) using a blender at maximum speed for 1 minute. Homogenates were differentially centrifuged at 10,000*g* (20 minutes) and 110,000*g* (60 minutes) at 4°C to obtain total (crude) membrane fractions. The final pellets were resuspended in 10% sucrose and 10 mM HEPES, pH 7.4, and aliquoted and stored at -80°C until needed.

Measurement of [^{3}H]Ryanodine and [^{3}H]PN200 Binding. Specific [^{3}H]ryanodine binding to RyR1 was assessed by incubating 100 μg/ml of crude microsomal preparations in buffer (in mM: 140 KCl, 10 NaCl, 20 HEPES, and 2 nM [^{3}H]ryanodine, pH 7.4) in the presence of 0–30 μM BPA or TBBPA and at optimal free Ca^{2+} conditions (50 μM total Ca^{2+}) without EGTA buffering. Nonspecific binding was assessed by adding 1000-fold (2 μM) excess unlabeled ryanodine. [^{3}H]Ryanodine binding experiments were performed at equilibrium conditions (3 hours at 37°C) with constant shaking (Cherednichenko et al., 2008). In competitive binding experiments, BPA or TCS was titrated in the presence of 0–30 μM TBBPA.

Specific [^{3}H]PN200 binding to DHPR was assessed by incubating 100 μg/ml of crude microsomal preparations in buffer (in mM: 140 NaCl, 15 KCl, 20 HEPES, and 2 nM [^{3}H]PN200, pH 7.1) in the presence of 0–30 μM BPA or TBBPA. Nonspecific binding was assessed by adding 5000-fold (10 μM) nifedipine. [^{3}H]PN200 binding experiments were performed in the dark at equilibrium conditions (1 hour at 25°C) with constant shaking.

All radioligand binding experiments were carried out in triplicate using two different membrane preparations, with final DMSO concentrations not exceeding 1% (v/v) (or 2% for competitive binding experiments). Binding reactions were quenched by rapid filtration through GF/B-grade glass fiber filters (Whatman, Clifton, NJ) using a harvester (Brandel, Gaithersburg, MD) with 5 ml of ice-cold binding buffer, and the filters were immersed in scintillation fluid (ScintiVerse BD Cocktail, Fisher Scientific, Waltham, MA). [^{3}H]Ryanodine and [^{3}H]PN200 retained in filters were quantified by liquid scintillation spectrometry using a Beckman Coulter LS6500 (Beckman Coulter, Indianapolis, IN). Specific binding of radioligand in the presence of BPA or TBBPA was calculated as percent change versus DMSO control, and binding curves were fit using nonlinear regression.

Measurement of Ca^{2+} Flux from SR Microsomes. Net Ca^{2+} efflux from actively loaded microsomal membrane vesicles was assessed spectrophotometrically using the metallochromic dye antipyrylazo-III (AP-III) by monitoring the absorbance at a wavelength of maximal absorbance of 710 nm with a UV-visible spectroscopy system (Agilent 8453, Agilent Technologies, Santa Clara, CA) (Feng et al., 1999). Crude membrane microsomal vesicles (100 μg/ml) were actively loaded in assay buffer (in mM: 0.25 AP-III, 92 KCl, 20 4-morpholinepropanesulfonic acid, 75 Na-pyrophosphate, pH 7.0) with three serial additions of 45 nmol of $CaCl_2$ in the presence of 1 mM MgATP, 4 mM phosphocreatine, and 10 μg/ml creatine phosphokinase. Once the AP-III signal returned to baseline, 0–30 μM BPA or TBBPA was added to the solution containing loaded vesicles to assess the compound's ability to trigger net Ca^{2+} release. For some experiments, pharmacologic blockade of RyR1 was achieved by preincubating the vesicles with 1 μM ruthenium red before the addition of compound. Absorbance signals were calibrated at the conclusion of each experiment by adding 1 μg of the Ca^{2+} ionophore A23187, followed by serial additions of 45 nmol of $CaCl_2$. Using this calibration, initial vesicular Ca^{2+} release rates as induced by BPA and TBBPA were calculated using linear regression of the initial 40 seconds of signal recorded after compound addition; total Ca^{2+} released was calculated from the overall change in absorbance after 5 minutes, converted to nmol Ca^{2+}, and expressed as a percentage of total Ca^{2+} loaded (135 nmol). All experiments were performed at 37°C with constant stirring.

Assessment of SERCA Activity. The activity of SERCA was measured using a coupled enzyme assay that monitors the rate of oxidation of NADH to NAD^+ at a wavelength of maximal absorbance of 340 nm with a UV-visible spectroscopy system. Crude membrane preparation (100 μg/ml) was added to the assay buffer (in mM: 100 KCl, 5 $MgCl_2$, 5 HEPES, 0.06 EGTA, 0.3 sucrose, 2 phosphoenolpyruvate, 0.1

$CaCl_2$, pH 7.2). In addition, the enzymes pyruvate kinase (8.7 U/ml) and lactate dehydrogenase (12.4 U/ml) were added to each reaction, along with 300 μM NADH as substrate. Once a stable absorbance signal at 340 nm was established, 0–30 μM BPA or TBBPA was added to the solution, and the biochemical reaction was initiated by the addition of 1 mM Na_2ATP. To relieve the SERCA pump of potential Ca^{2+} back pressure caused by activation of RyR1, each reaction was supplemented with 1 μg of the Ca^{2+} ionophore A23187. The SERCA inhibitor thapsigargin (1 μM) was added to the positive control to assess the non-SERCA component of ATPase activity. SERCA activity was derived from the maximum rate of NADH conversion achieved over a 1-minute period, with the corresponding non-SERCA rate subtracted out. Modulation of SERCA activity by BPA or TBBPA was expressed as percentage of DMSO control. All experiments were performed at 37°C with constant stirring and using two different membrane preparations.

Preparation and Culture of Primary Myotubes. Primary skeletal myoblasts were isolated from mixed-sex wild-type mouse neonates, as previously described (Rando and Blau, 1994). Specifically, myoblasts were cultured in 10-cm tissue culture–treated dishes coated with calf-skin collagen in Ham's F-10 medium supplemented with 20% (v/v) HyClone bovine growth serum (GE Healthcare Life Sciences, Logan, UT), 2 mM L-glutamine, 100 IU/ml penicillin G, 100 μg/ml streptomycin sulfate, and 4 ng/ml basic fibroblast growth factor (PeproTech, Rocky Hill, NJ) at 37°C in 5% CO_2/10% O_2. For Ca^{2+} imaging experiments, myoblasts were seeded onto Matrigel-coated 96-well imaging plates; for resting membrane potential measurements, myoblasts were seeded onto Matrigel-coated 35-mm tissue culture–treated dishes. Upon reaching ~80% confluency (1.5×10^4 cells/well or 3.0×10^5 cells/dish), growth factor was withdrawn, and the myoblasts were allowed to differentiate into myotubes for 3 to 4 days in Dulbecco's modified Eagle's medium containing 5% (v/v) heat-inactivated horse serum (Invitrogen, Waltham, MA), 2 mM L-glutamine, 100 IU/ml penicillin G, and 100 μg/ml streptomycin sulfate at 37°C in 5% CO_2/10% O_2.

Imaging of Ca^{2+} Transients in Differentiated Myotubes. Skeletal myotubes were loaded with the fluorescent Ca^{2+} indicator fluo-4-acetoxy-methyl ester and imaged using a cooled charge-coupled device camera with a 40× objective. Cells were illuminated at 488 nm using a DeltaRam excitation source (Photon Technology International, Lawrenceville, NJ), and fluorescence emission was captured at 510 nm from regions of interest at 30 frames per second; recorded images were digitized and analyzed using EasyRatioPro software (Photon Technology International). Electrical field stimulation was applied using two platinum electrodes attached to opposite sides of the well and connected to a Master-8 programmable pulse stimulator (A.M.P.I., Jerusalem, Israel), delivering 7 V, 25 millisecond bipolar pulses. Continuous twitch responses were maintained at 0.1 Hz, whereas staircase responses were elicited through preprogrammed 5-second pulse trains from 1 to 40 Hz. After acquiring 3–5 minutes of initial baseline recordings, BPA (30 μM), TBBPA (1–10 μM), or control (0.1% DMSO) was delivered by bulk perfusion in Tyrode's solution (in mM: 140 NaCl, 5 KCl, 2 $MgCl_2$, 10 HEPES, 10 glucose, 2 $CaCl_2$, pH 7.3). The cells were challenged by caffeine (Caff, 20 mM) by brief focal application using a micropipette. For subacute experiments, myotubes were exposed to submicromolar TBBPA for 24 hours in serum-free Dulbecco's modified Eagle's medium. Transient amplitude was calculated for each peak by normalizing the peak change in fluo-4 fluorescence ($F_{max} - F_0$, or ΔF) to the baseline fluorescence preceding the peak (F_0) and is presented as $\Delta F/F_0$. The full width at half maximum for Ca^{2+} transients was determined as the time elapsed between achieving ½ΔF on the upstroke and down stroke of the transient. For all experiments, data were obtained from cells over at least three different experimental days.

Measurement of Myotube Resting Membrane Potential. Skeletal myotube resting membrane potential (V_m) was directly assessed by impalement using glass microelectrodes. Thin-wall (1.5 mm/1.12 mm o.d./i.d.) glass capillaries with filament (World Precision Instruments, Sarasota, FL) were pulled using a P-87 micropipette puller (Sutter Instrument, Novato, CA) to fabricate microelectrodes with a long taper and submicron tip with resistance between 12 and 18 MΩ. Each microelectrode was filled with a 3 M solution of KCl before the experiment. V_m signals were acquired and filtered using a high impedance amplifier (Duo 773, World Precision Instruments) and subsequently digitized using a Digidata 1440A (Molecular Devices, Sunnyvale, CA); recorded data were analyzed using pClamp 10 software suite (Molecular Devices). For each dish, five initial measurements were made in normal Tyrode's solution, and an additional 10 measurements were made 10 minutes after adding BPA (30 μM), TBBPA (10 μM), or control (0.1% DMSO) to the cells. For the initial measurements, myotubes with V_m less negative than -60 mV were rejected for potential membrane damage (<15% of myotubes). All impalements were performed on independent myotubes, and data were collected from three different culture days.

Statistical Analysis. All data are presented as mean ± S.E.M., and all error bars represent S.E.M. All best-fit EC_{50}/IC_{50} values are reported with corresponding 95% confidence intervals (CI). Where appropriate, comparisons were made using one-way analysis of variance (ANOVA) with Dunnett's post hoc test or two-way ANOVA with Dunnett's post hoc test; $P < 0.05$ was considered significant. All curve-fitting (linear and nonlinear) and statistical tests were accomplished using GraphPad Prism (GraphPad Software, La Jolla, CA).

Results

TBBPA, but not BPA, Engages Targets that Alter Ca^{2+} Flux Equilibrium. Skeletal muscle ECC invariably relies on the participation and function of RyR1 and DHPR. We examined whether BPA and TBBPA directly modulate the activity of RyR1—and potentially disrupt the physiologic process of ECC. The binding of [^{3}H]ryanodine to RyR1 is a conformationally sensitive process in which an increase in specific radioligand binding is indicative of increased RyR1 Ca^{2+} channel activity (Pessah et al., 1987). TBBPA elicited a concentration-dependent increase in specific [^{3}H]ryanodine binding to RyR1 (EC_{50} = 7.7 μM, 95% CI: 6.8–8.8 μM; Fig. 1A, top), achieving 352.5 ± 12.1% and 463.6 ± 12.5% of control at 10 and 30 μM, respectively (Fig. 1A, bottom), suggesting that TBBPA stabilizes the open conformation of RyR1. By comparison, BPA (30 μM) elicited a modest yet significant increase in [^{3}H]ryanodine binding (140.4% ± 7.5% of control; Fig. 1A, bottom).

We observed a similar divergence in the ability of BPA and TBBPA to interact with DHPR. As the conformationally coupled partner of RyR1 in skeletal muscle ECC, DHPR also conducts the dihydropyridine-sensitive L-type Ca^{2+} current; displacement of the high-affinity ligand [^{3}H]PN200 from DHPR by a compound would indicate interactions at the dihydropyridine binding site and consequent inhibition of the associated L-type Ca^{2+} current. TBBPA's potent targeting of DHPR reduced specific [^{3}H]PN200 binding (IC_{50} = 1.2 μM, 95% CI: 1.0–1.4 μM; Fig. 1B, top), resulting in complete abrogation of radioligand binding at 10 μM (Fig. 1B, bottom); in contrast, BPA had no inhibitory effects up to 30 μM (Fig. 1B).

Complementary to ECC in skeletal muscle function is the relaxation process, which is mediated, among others, by SERCA, which pumps cytosolic Ca^{2+} back into the SR. Using a spectrophotometric assay that couples NADH oxidation to ATP hydrolysis by SERCA, we examined the activity of this enzyme by quantifying the rate of change in NADH absorbance. TBBPA altered SERCA activity in a non-monotonic manner (Fig. 2, A and C). TBBPA significantly increased

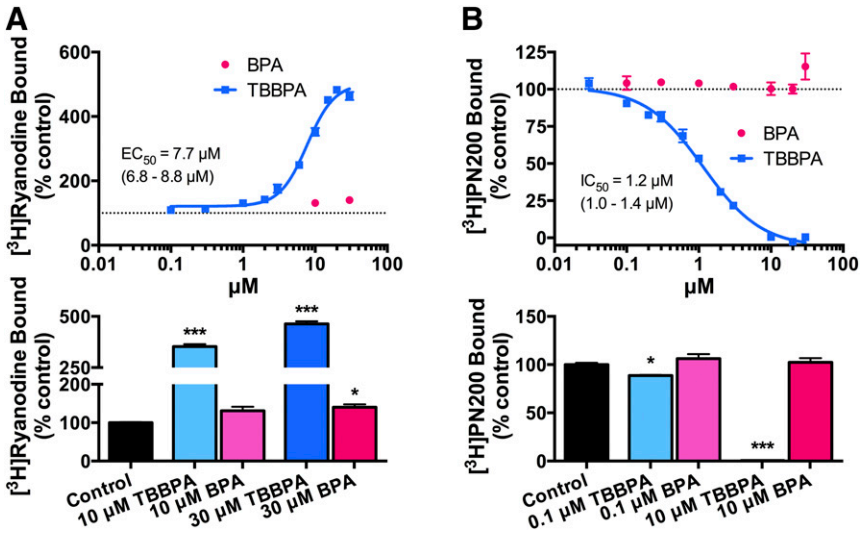

Fig. 1. Radioligand binding to integral players of skeletal muscle ECC in the presence of BPA and TBBPA. (A) Skeletal muscle microsomal preparations were incubated with [^{3}H]ryanodine and BPA or TBBPA to assess modulation of RyR1 activity. Bottom panel shows comparison of specific [^{3}H]ryanodine binding to RyR1 as induced by BPA and TBBPA (10, 30 μM). (B) Skeletal muscle microsomal preparations were incubated with [^{3}H]PN200 and BPA or TBBPA to determine interactions at the dihydropyridine binding site. Bottom panel shows comparison of specific [^{3}H]PN200 binding to DHPR as modified by BPA and TBBPA (0.1, 10 μM). Data represent mean ± S.E.M., performed in triplicate. Values in parentheses represent the 95% CI of the EC_{50}/IC_{50}. $^*P \leq 0.05$; $^{***}P \leq 0.001$ compared with control group (one-way ANOVA with Dunnett's post-test).

SERCA activity ($P \leq 0.05$, one sample t test) at all concentrations tested below 10 μM, achieving 143.8% ± 7.2% of control at 6 μM, whereas the effect became inhibitory ≥10 μM (overall IC_{50} = 13.3 μM; 95% CI: 10.2–17.4 μM). BPA exerted no impact on SERCA activity up to 30 μM (Fig. 2A).

Microsomal Ca^{2+} fluxes are a dynamic process reflecting the overall balance between Ca^{2+} release via RyR1 and active reuptake via SERCA. Congruent with predictions from [^{3}H]ryanodine binding and SERCA activity measurements, TBBPA elicited a concentration-dependent efflux of actively accumulated Ca^{2+} from microsomal vesicles (EC_{50} = 6.5 μM, 95% CI: 4.1–10.5 μM; Fig. 2B, traces *d–f*), which was sensitive to inhibition by the RyR1 blocker ruthenium red (Fig. 2B, trace *h*). In contrast, 30 μM BPA was unable to induce a net Ca^{2+} efflux from vesicles in the presence of SERCA activity (Fig. 2B, trace *i*). Figure 2C summarizes the relative concentration-effect relationships for SERCA inhibition and RyR1 activation for TBBPA, two mutually enforcing mechanisms predicted to be highly disruptive of ECC in skeletal muscle.

Both BPA and TBBPA Disrupt ECC in Intact Skeletal Myotubes. Based on TBBPA's target engagement of RyR1, DHPR, and SERCA, we hypothesized a potent adverse impact on ECC in intact embryonic muscle. As a corollary, we anticipated BPA to be without effect. Perfusion of 10 μM TBBPA onto skeletal myotubes caused a robust transient rise in cytoplasmic Ca^{2+} accompanied by loss of electrical responsiveness that became complete within 20 minutes despite partial recovery of Ca^{2+} baseline (Fig. 3, second trace; Fig. 4A). After 20 minutes, 1 μM TBBPA reduced transient amplitudes by 35.6% ± 3.3% (Fig. 3, third trace; Fig. 4A). Unexpectedly, 30 μM BPA (a concentration that had minimal or no effects on the trio of ECC protein targets tested) altered myotube Ca^{2+} dynamics, with cells responding in two distinctly different patterns classified as type I (45% of cells), whose Ca^{2+} transient amplitudes decreased but were not abolished (similar to 1 μM TBBPA), and type II (55% of cells), in which Ca^{2+} transients rapidly extinguished after perfusion of BPA (Fig. 3, fourth and fifth traces; Fig. 4A shows a composite summary for both BPA effect types). Washout of BPA rapidly restored

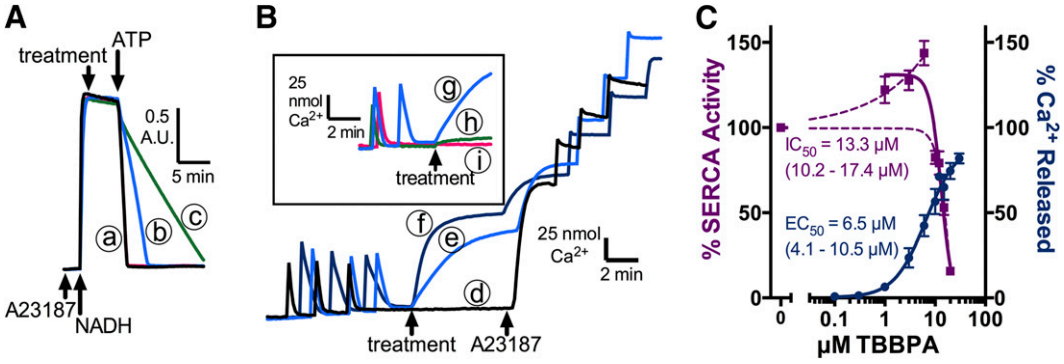

Fig. 2. Modification of microsomal Ca^{2+} fluxes as effected by BPA and TBBPA. (A) SERCA activity in the presence of BPA or TBBPA was assessed using an enzyme system coupling ATP hydrolysis to NADH oxidation and monitored at a wavelength of maximal absorbance (λ_{max}) of 340 nm. (a) Control and 30 μM BPA; (b) 20 μM TBBPA; (c) SERCA inhibitor thapsigargin (TG). (B) Skeletal muscle microsomes were actively loaded with Ca^{2+} in the presence of ATP and the Ca^{2+} indicator AP-III, and BPA or TBBPA was applied following the loading phase. (d) Control; (e) 10 μM TBBPA; (f) 30 μM TBBPA; (g) 10 μM TBBPA; (h) 10 μM TBBPA + ruthenium red (RR, RyR1 inhibitor); (i) 30 μM BPA. (C) Summary of the concentration-dependent effects of TBBPA on Ca^{2+} release (n = 3 or 4) and SERCA activity (n = 7) in skeletal microsomes. For SERCA activity, dashed curves represent separately the activating and inhibitory components; the solid line represent the overall concentration-response relationship. Data represent mean ± S.E.M. Values in parentheses represent the 95% CI of the EC_{50}/IC_{50}.

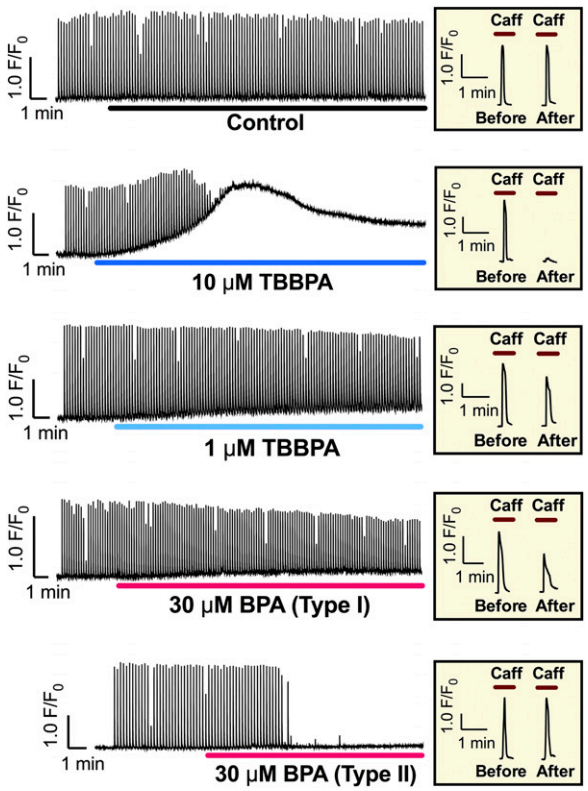

Fig. 3. Representative imaging traces showing dysregulation of Ca^{2+} dynamics by both BPA and TBBPA in intact skeletal myotubes. Skeletal myotubes were loaded with the fluorescent Ca^{2+} indicator fluo-4 and continuously stimulated at 0.1 Hz while vehicle, BPA (30 μM), or TBBPA (1 or 10 μM) was applied by perfusion after the initial baseline recording. Caff (20 mM) was briefly applied both before and after perfusion of compound. Of note, 30 μM BPA produced two distinct types of effects on myotube Ca^{2+} dynamics.

Ca^{2+} transients in a subset of cells, whereas the effects of TBBPA were invariably irreversible (data not shown).

TBBPA slowed Ca^{2+} transient kinetics, nearly doubling the full width at half maxima of peaks at 1 μM and prolonging transient widths to 335.2% ± 34.0% of baseline after 20 minutes (Fig. 4B). In contrast, 30 μM BPA did not significantly modify peak widths.

TBBPA Disrupts Ca^{2+} Homeostasis in Myotubes. To test our assertion that TBBPA alters intracellular Ca^{2+} regulation in skeletal myotubes, we analyzed both the change in baseline Ca^{2+} and the filling state of SR Ca^{2+} stores after exposure. TBBPA concentration dependently increased baseline Ca^{2+} (to 186.9% ± 8.7% of initial baseline after 20 minutes at 10 μM), whereas BPA (both response types) had minimal effects on this parameter (Fig. 4C).

Because depletion of SR Ca^{2+} stores can lead to ECC failure in skeletal myotubes, we interrogated the state of the stores by quantifying the amplitude of the postexposure Caff response relative to a similar challenge before exposure. Although Caff does not completely deplete the SR of Ca^{2+}, this challenge nonetheless provides a gross estimation of the filling state of the SR. Consistent with prior observations, 10 μM TBBPA produced a severe depletion of SR stores as indicated by an 82.6% ± 2.3% lower postexposure Caff response, whereas a much milder depletion was observed with 30 μM BPA (13.1% ± 8.2% decrease) (Fig. 4D). Although type II responding cells for BPA exhibited greater SR Ca^{2+} content versus type I cells, this difference was not significant (data not shown).

BPA and TBBPA Modify V_m in Opposing Directions. We explored the possibility of BPA and TBBPA altering skeletal myotube V_m as an auxiliary mechanism by which these compounds impair muscle function. Measurements of membrane potential were recorded from myotubes using submicron tip microelectrodes before and after exposure to 30 μM BPA and 10 μM TBBPA, concentrations that rapidly attenuated Ca^{2+} transients. Cells exposed to vehicle retained a V_m of -62.1 ± 0.2 mV that was stable for at least 10 minutes. Treatment with BPA caused a significant hyperpolarization of V_m to -67.6 ± 0.6 mV, whereas TBBPA significantly depolarized V_m to -52.6 ± 0.9 mV (Fig. 4E).

Subacute TBBPA Exposure Diminishes Ca^{2+} Responses in Myotubes. Whereas acute doses may provide insight into the molecular targets and mechanisms by which TBBPA disrupts skeletal ECC, lower and more prolonged doses may better reflect realistic human exposures to this chemical. To this end, we implemented a subacute (24-hour) exposure protocol with skeletal myotubes at submicromolar concentrations of TBBPA. Congruent with our findings in the acute exposure paradigm, 500 nM TBBPA significantly reduced all Ca^{2+} transient amplitudes as evoked by 1- to 40-Hz electrical stimuli (responses ranged from 81.4% ± 2.7% to 85.2% ± 2.8% of control response within each stimulation frequency); a significant reduction was also seen with 100 nM TBBPA at 40 Hz (90.5% ± 2.7% of control; Fig. 5A). Furthermore, 500 nM TBBPA significantly reduced SR Ca^{2+} stores after 24 hours as indicated by a 13.9% ± 3.0% smaller Caff response versus control (Fig. 5B).

Interactions between TBBPA and TCS on [^{3}H]Ryanodine Binding. The acute effects of TBBPA observed in skeletal myotubes were reminiscent of our previous findings in myotubes with the bactericidal chemical TCS (Cherednichenko et al., 2012; Fritsch et al., 2013). We therefore hypothesized a common mechanism for these two environmental contaminants. To test this, we assessed whether titration of TCS influenced TBBPA's concentration-response relationship in the [^{3}H]ryanodine binding assay. Increasing concentrations of TCS (1–10 μM) mitigated the activating effect of TBBPA at RyR1; normalized to control, 10 μM TCS reduced the efficacy of 30 μM TBBPA by ~50% (Fig. 6A). Additionally, 10 μM TCS produced a significant shift in the potency of TBBPA from an EC_{50} of 11.6 μM (95% CI: 9.3–14.5 μM) to 5.1 μM (95% CI: 3.5–7.3 μM). Moreover, increasing the concentration of TCS to 30 μM reversed the excitatory effect of TBBPA (IC_{50} = 22.5 μM, 95% CI: 9.0–56.4 μM), ultimately reducing specific [^{3}H]ryanodine binding at 30 μM TBBPA to 38.1% ± 3.0% of control. In contrast, no significant interaction between TBBPA and BPA was observed using [^{3}H]ryanodine binding (Fig. 6B).

Discussion

In this present study, we investigated the effects of BPA and TBBPA on Ca^{2+} dynamics and signaling in embryonic skeletal muscle and the mechanistic divergence between these two compounds afforded by their structural differences. In contrast to previous studies of the endocrine disrupting properties of BPA and TBBPA, we identify here new molecular targets within the sarcolemma and SR that impair ECC in developing

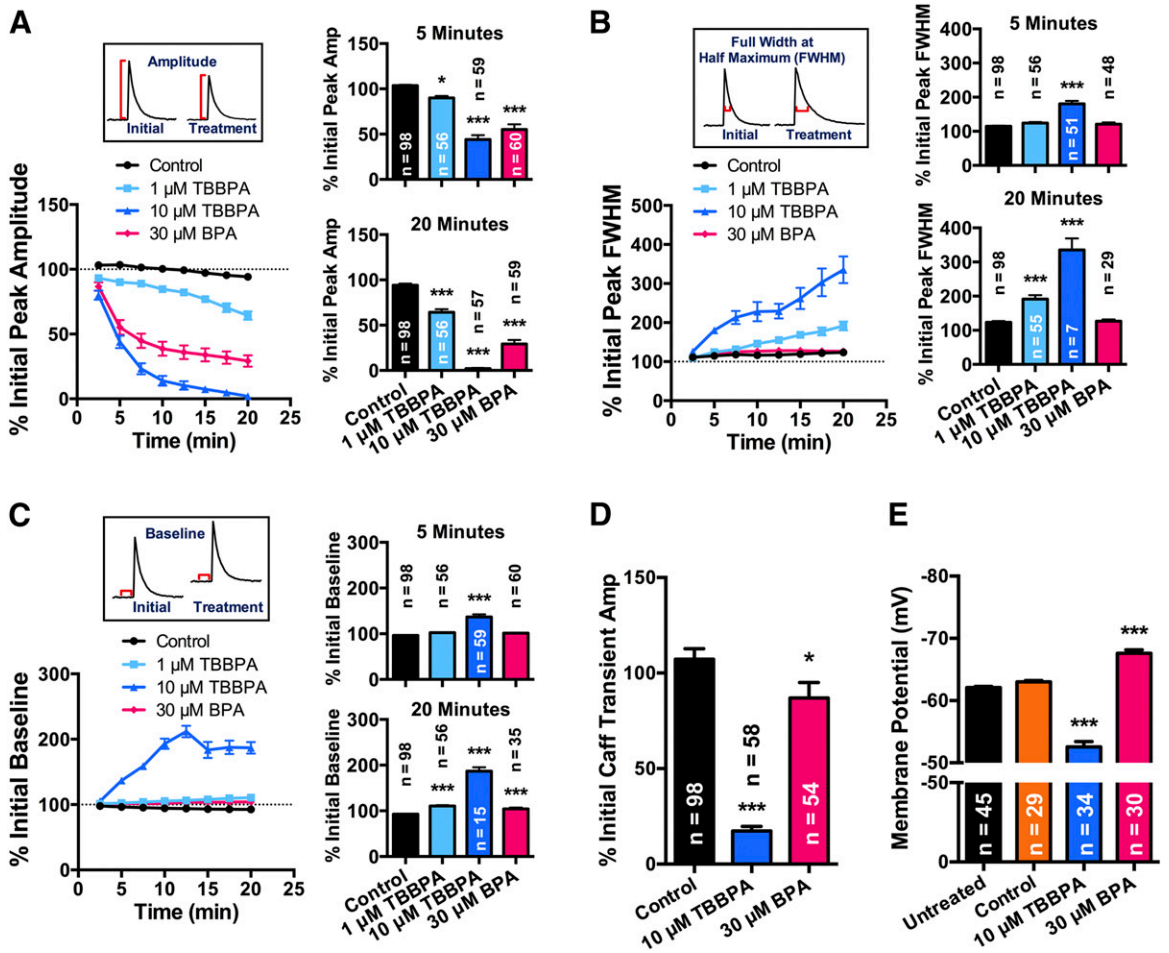

Fig. 4. Functional alterations induced by BPA and TBBPA in skeletal myotubes. (A–C) Effects of BPA and TBBPA on evoked Ca^{2+} transients (visualized by fluorescent Ca^{2+} imaging), specifically, changes in (A) transient amplitude (Amp), (B) transient full width at half maximum (FWHM), and (C) baseline fluorescence (insets represent the quantification method for these parameters). The respective right panels show comparisons between conditions after 5 (top) and 20 (bottom) minutes of compound perfusion, where decreases in *n* are due to the loss of response to electrical stimulation. (D) The amplitude of the Caff transient after the BPA or TBBPA exposure protocol, as normalized to a similar challenge before compound addition. (E) The V_m of myotubes, assessed through microelectrode impalement, both before (untreated) and after 10 minutes of exposure to vehicle, BPA, or TBBPA. Data represent mean ± S.E.M. Individual *n* values are reported in each panel. $^*P \leq 0.05$; $^{***}P \leq 0.001$ compared with control group (one-way ANOVA with Dunnett's post-test). All BPA data shown are composites of both observed effect types.

skeletal muscle. Although BPA and TBBPA differ merely in bromination, only TBBPA targets proteins critical for physiologic ECC, with a rank potency of DHPR > RyR1 > SERCA (summarized in Fig. 7). Nevertheless, there is a convergence with respect to these chemicals' ability to disrupt function at the cellular level. BPA's unexpected capacity to impair myotube ECC, albeit with lower potency than TBBPA, appears to be related to cell hyperpolarization that dampens membrane excitability absent of any interactions with DHPR, RyR1, and SERCA.

TBBPA's ability to enhance RyR1 activity and inhibit SERCA has broad implications on skeletal muscle function since these two actions result in a feed-forward manner to shift Ca^{2+} from SR stores into the sarcoplasm that quickly results in ECC failure (Fig. 4, C and D). This elevation of resting $[Ca^{2+}]_i$ is not only implicated in muscle fatigue (Verburg et al., 2006) but can also produce untoward cellular effects over prolonged periods. Indeed, previous studies have shown TBBPA to elicit a mobilization of Ca^{2+} and induce death in neuronal and testicular cell types (Reistad et al., 2007; Ogunbayo et al., 2008; Hendriks et al., 2012). The role of RyR1 in mediating this $[Ca^{2+}]_i$ elevation was suggested in a previous work through pharmacologic inhibition (Ogunbayo et al., 2008), but our results unequivocally demonstrate a direct modulation of RyR1 activity through radioligand binding and SR flux experiments. TBBPA's actions on RyR1 are further highlighted in the competition binding studies with TCS, a compound previously shown to impair skeletal ECC through interactions with RyR1 (Cherednichenko et al., 2012). The modification by TCS on the efficacy of TBBPA on [^{3}H]ryanodine binding (Fig. 6) strongly suggests a noncompetitive interaction between these two structurally related high-volume chemicals when engaging RyR1, arising perhaps from mutually exclusive binding sites that allosterically modify channel activity.

Previous studies have also reported TBBPA to have inhibitory effects on SERCA in skeletal muscle preparations (Ogunbayo and Michelangeli, 2007; Ogunbayo et al., 2008) but with higher potency than our findings (1.2–1.7 μM vs. 13.3 μM); this discrepancy may be attributed to variations in lipid content that can alter the bioavailability of TBBPA through adsorption. The lack of activity of BPA on SERCA

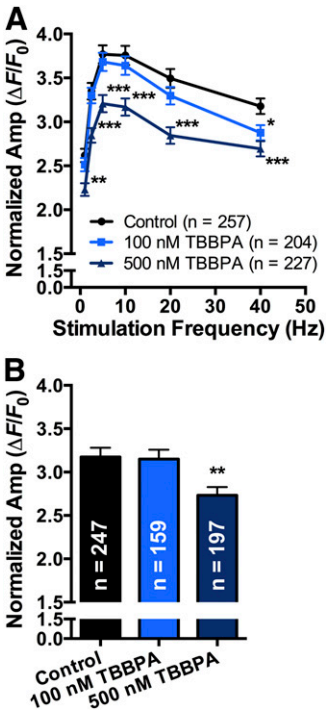

Fig. 5. Functional changes visualized by fluorescent Ca^{2+} imaging after 24-hour exposure to submicromolar TBBPA in skeletal myotubes. (A) Transient amplitudes (normalized to baseline fluorescence) in response to 1- to 40-Hz electrical stimuli. (B) Normalized amplitude of transient induced by Caff challenge. Data represent mean ± S.E.M. Individual n values are reported in each panel. $^*P \leq 0.05$; $^{**}P \leq 0.01$; $^{***}P \leq 0.001$ compared with control group [two-way ANOVA with Dunnett's post-test comparing to control at each frequency (A); one-way ANOVA with Dunnett's post-test (B)].

activity is consistent with a previous report in skeletal muscle microsomes (Woeste et al., 2013), yet it contradicts a submicromolar potency finding using rat testis microsomes (Hughes et al., 2000). This could be explained by expressional differences in SERCA such that SERCA1a, the dominant isoform in fast twitch muscle, may either be more resistant per se or compensated through higher expression density compared with the isoform(s) in nonmuscle cells (Periasamy and Kalyanasundaram, 2007). The SERCA-activating effect of TBBPA <10 μM in the presence of ionophore may suggest cross-talk between SERCA and RyR1 as previously posited (Gilchrist et al., 2003).

Beyond the SR, it is evident that TBBPA has additional targets in the sarcolemma, as demonstrated by its displacement of [^{3}H]PN200 from DHPR. Although not a functional assessment of L-type Ca^{2+} current, it is reasonable to believe that this potent interaction at the dihydropyridine binding site translates to a loss of Ca^{2+} current mediated by DHPR (Zamponi et al., 2015). Finally, the depolarization induced by TBBPA suggests target(s) on the sarcolemma that determine resting V_m, such as K^+ or Cl^- channels, either through direct interactions or Ca^{2+}-mediated mechanisms.

The involvement of RyR in BPA-induced Ca^{2+} dysregulation has previously been determined in murine cardiomyocytes, although involving downstream influences of estrogen receptor signaling (Yan et al., 2011; Gao et al., 2013); however, the contribution of nonestrogenic pathways in BPA's impairment of ECC cannot be discounted considering our radioligand binding findings with BPA. Although mild, the significant increase in specific [^{3}H]ryanodine binding at 30 μM may highlight a possible mechanism for the observed type I effect. The dichotomy of Ca^{2+} responses with BPA may be driven by cellular heterogeneity consequent of varying degrees of myotube differentiation. Emerging evidence indicates that BPA interacts promiscuously with a wide range of ion channels in both excitable and nonexcitable cells (Soriano et al., 2016). Several studies have shown BPA to alter cellular excitability mediated through a range of actions, including activating the large conductance Ca^{2+}/voltage-gated K^+ channels in coronary smooth muscle cells (Asano et al., 2010), inhibiting the cardiac (O'Reilly et al., 2012) and neuronal (Wang et al., 2011) isoforms of voltage-gated Na^+ channels, and modifying a spectrum of voltage-gated Ca^{2+} channels, including L-, N-, P/Q-, R-, and

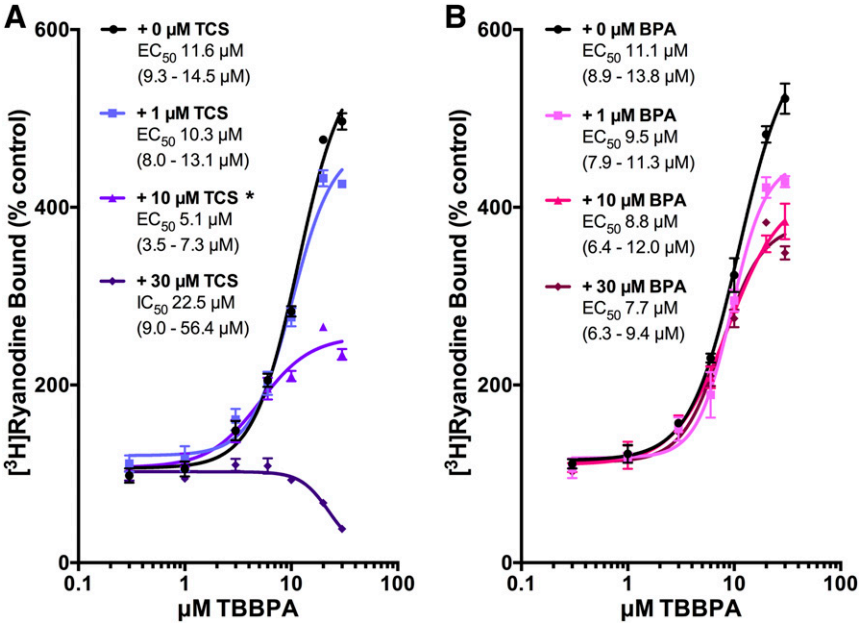

Fig. 6. The concentration-response relationship of TBBPA on specific [^{3}H]ryanodine binding to RyR1 in the additional presence of either (A) TCS or (B) BPA. Data represent mean ± S.E.M., performed in triplicate. Values in parentheses represent the 95% CI of the EC_{50}/IC_{50}. $^*P \leq 0.05$ compared with EC_{50} of control group (TBBPA alone) (one-way ANOVA with Dunnett's post-test).

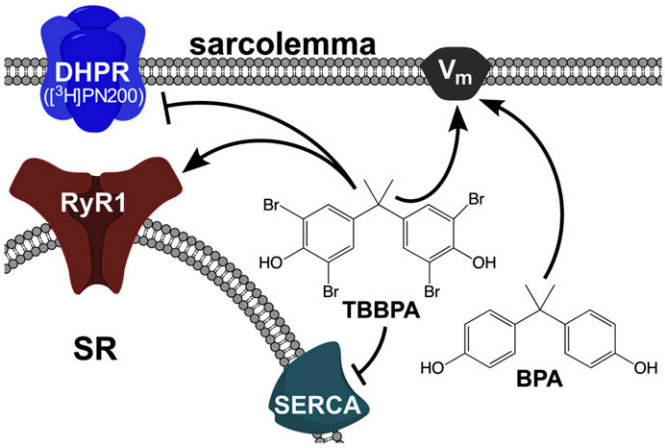

	RyR1	DHPR	SERCA	V_m
BPA	Mild Activator	No Interaction	No Interaction	Hyper-polarizing
TBBPA	Strong Activator	Strong Inhibitor	Mild Inhibitor	Depolarizing

Fig. 7. Scheme summarizing the interactions of BPA and TBBPA with new targets identified in this study leading to skeletal muscle dysfunction. The nature and degree of target engagement by the two compounds are summarized in the accompanying table.

T-type channels (Pandey and Deshpande, 2012; Deutschmann et al., 2013; Wang et al., 2013; Michaela et al., 2014). One or more of these mechanisms could account for how BPA impairs ECC in myotubes, leading to a type II loss of function, and is consistent with the hyperpolarizing influence of BPA observed in the current investigation.

Although our findings illustrate a mechanism of muscle impairment independent of endocrine-related signaling pathways, further engagement of estrogen and thyroid receptor pathways by BPA and TBBPA, respectively, present a feed-forward mechanism that can exacerbate skeletal muscle dysfunction. Both estrogen and thyroid receptors have been shown to be critical players in, among other things, glucose homeostasis and repair processes in skeletal muscle (Enns and Tiidus, 2010; Barros and Gustafsson, 2011; Salvatore et al., 2014). Since skeletal muscle is a well perfused organ that constitutes 30%–40% of body mass in humans, dysregulation of these fundamental processes can have far-reaching consequences throughout the entire body. Concurrent engagement of endocrine and nonendocrine pathways by exogenous chemicals, such as BPA and TBBPA, can therefore produce mutually destabilizing effects that ultimately compromise the function and health of muscle.

Knowledge gained from our study ultimately serves two ends: 1) to understand the structural requisites for forming molecular interactions with proteins critical for skeletal muscle Ca^{2+} regulation and function; 2) to differentiate molecular targets of BPA and TBBPA. The protein players investigated here—DHPR, RyR, and SERCA—have isoforms that are widely expressed beyond skeletal muscle, and the modification of their function in tissues such as neurons and cardiac muscle can have broad implications. Our findings regarding TBBPA have not only revealed new biologic targets for this high-volume chemical but, importantly, demonstrate that its multiple modes of action translate to a detectable diminution of a fundamentally important physiologic process at a threshold concentration of 100 nM after subacute exposure in primary myotubes. This concentration [~50 parts per billion (ppb)] is in line with those detected in human samples—up to 10 ppb in serum lipid (Kim and Oh, 2014)—and is exceeded by levels detected in occupational settings, roughly 100–10,000 ppb in solid waste and dust (Zhou et al., 2014). That neonates have been detected to have up to 83 ppb TBBPA in serum lipid (Kim and Oh, 2014) highlights this special population as especially vulnerable to BPA and TBBPA exposure owing to immature metabolism pathways. Urinary BPA concentrations have similarly been reported to be higher in premature infants compared with healthy children and adults (Calafat et al., 2008, 2009). These findings of elevated TBBPA and BPA concentrations in newborns harmonize with our use of an embryonic form of primary skeletal muscle for assessing Ca^{2+} dysregulation. The loss of muscle strength and tone, as predicted by our myotube model, not only affects mobility and movement but—of particular importance to the developing infant—can produce more enduring effects by perturbing transcriptional pathways innately regulated by $[Ca^{2+}]_i$ that are necessary for, among others, myogenesis (Gundersen, 2011). In extreme cases, neonatal hypotonia resulting from disorders such as muscular dystrophy can impair feeding and respiration, as well as cause muscle wasting (Emery, 2002; Sparks, 2015). More work is needed to determine whether prolonged exposures to BPA and TBBPA can lead to similar detriments to muscle and developmental physiology in the whole organism.

In this study, we demonstrate for the first time the deleterious effects of BPA and TBBPA exposure on skeletal muscle function. Exposure to both chemicals is toxicologically relevant and concerning because of their high production volume and ubiquitous inclusion into consumer products worldwide. Our findings add to the growing knowledge base on the chemistry of RyR1 modulation while ultimately linking TBBPA to other tissue toxicities through a common mechanism of DHPR, RyR, and SERCA dysregulation. Furthermore, that BPA impairs skeletal muscle function without engaging these molecular targets implies a distinct mechanism of action that may involve instead the modulation of cellular excitability. Understanding the spectrum of targets of BPA and TBBPA is critical for reducing the risks of these ubiquitous chemicals and limiting toxic, and especially chronic, exposures. As newer alternatives are developed to replace these compounds (Ezechiáš et al., 2014; Rosenmai et al., 2014), it is paramount to scrutinize the structural properties of these replacements to ensure that they are safe for everyday consumer use.

Authorship Contributions

Participated in research design: Zhang, Pessah.
Conducted experiments: Zhang.
Contributed new reagents or analytic tools: Zhang, Pessah.
Performed data analysis: Zhang.
Wrote or contributed to the writing of the manuscript: Zhang, Pessah.

References

Asano S, Tune JD, and Dick GM (2010) Bisphenol A activates Maxi-K (K(Ca)1.1) channels in coronary smooth muscle. *Br J Pharmacol* **160**:160–170.
Barros RP and Gustafsson JA (2011) Estrogen receptors and the metabolic network. *Cell Metab* **14**:289–299.
Birnbaum LS and Staskal DF (2004) Brominated flame retardants: cause for concern? *Environ Health Perspect* **112**:9–17.

Calafat AM, Weuve J, Ye X, Jia LT, Hu H, Ringer S, Huttner K, and Hauser R (2009) Exposure to bisphenol A and other phenols in neonatal intensive care unit premature infants. *Environ Health Perspect* **117**:639–644.

Calafat AM, Ye X, Wong LY, Reidy JA, and Needham LL (2008) Exposure of the U.S. population to bisphenol A and 4-tertiary-octylphenol: 2003-2004. *Environ Health Perspect* **116**:39–44.

Cherednichenko G, Ward CW, Feng W, Cabrales E, Michaelson L, Samso M, López JR, Allen PD, and Pessah IN (2008) Enhanced excitation-coupled calcium entry in myotubes expressing malignant hyperthermia mutation R163C is attenuated by dantrolene. *Mol Pharmacol* **73**:1203–1212.

Cherednichenko G, Zhang R, Bannister RA, Timofeyev V, Li N, Fritsch EB, Feng W, Barrientos GC, Schebb NH, Hammock BD, et al. (2012) Triclosan impairs excitation-contraction coupling and Ca2+ dynamics in striated muscle. *Proc Natl Acad Sci USA* **109**:14158–14163.

Deutschmann A, Hans M, Meyer R, Häberlein H, and Swandulla D (2013) Bisphenol A inhibits voltage-activated Ca(2+) channels in vitro: mechanisms and structural requirements. *Mol Pharmacol* **83**:501–511.

Emery AE (2002) The muscular dystrophies. *Lancet* **359**:687–695.

Enns DL and Tiidus PM (2010) The influence of estrogen on skeletal muscle: sex matters. *Sports Med* **40**:41–58.

Ezechiáš M, Covino S, and Cajthaml T (2014) Ecotoxicity and biodegradability of new brominated flame retardants: a review. *Ecotoxicol Environ Saf* **110**:153–167.

Feng W, Liu G, Xia R, Abramson JJ, and Pessah IN (1999) Site-selective modification of hyperreactive cysteines of ryanodine receptor complex by quinones. *Mol Pharmacol* **55**:821–831.

Fritsch EB, Connon RE, Werner I, Davies RE, Beggel S, Feng W, and Pessah IN (2013) Triclosan impairs swimming behavior and alters expression of excitation-contraction coupling proteins in fathead minnow (Pimephales promelas). *Environ Sci Technol* **47**:2008–2017.

Gao X, Liang Q, Chen Y, and Wang HS (2013) Molecular mechanisms underlying the rapid arrhythmogenic action of bisphenol A in female rat hearts. *Endocrinology* **154**:4607–4617.

Gilchrist JS, Palahniuk C, Abrenica B, Rampersad P, Mutawe M, and Cook T (2003) RyR1/SERCA1 cross-talk regulation of calcium transport in heavy sarcoplasmic reticulum vesicles. *Can J Physiol Pharmacol* **81**:220–233.

Gundersen K (2011) Excitation-transcription coupling in skeletal muscle: the molecular pathways of exercise. *Biol Rev Camb Philos Soc* **86**:564–600.

Hendriks HS, van Kleef RG, van den Berg M, and Westerink RH (2012) Multiple novel modes of action involved in the in vitro neurotoxic effects of tetrabromobisphenol-A. *Toxicol Sci* **128**:235–246.

Hughes PJ, McLellan H, Lowes DA, Kahn SZ, Bilmen JG, Tovey SC, Godfrey RE, Michell RH, Kirk CJ, and Michelangeli F (2000) Estrogenic alkylphenols induce cell death by inhibiting testis endoplasmic reticulum Ca(2+) pumps. *Biochem Biophys Res Commun* **277**:568–574.

Johnson-Restrepo B, Adams DH, and Kannan K (2008) Tetrabromobisphenol A (TBBPA) and hexabromocyclododecanes (HBCDs) in tissues of humans, dolphins, and sharks from the United States. *Chemosphere* **70**:1935–1944.

Kang JH, Kondo F, and Katayama Y (2006) Human exposure to bisphenol A. *Toxicology* **226**:79–89.

Kim UJ and Oh JE (2014) Tetrabromobisphenol A and hexabromocyclododecane flame retardants in infant-mother paired serum samples, and their relationships with thyroid hormones and environmental factors. *Environ Pollut* **184**:193–200.

Michaela P, Mária K, Silvia H, and L'ubica L (2014) Bisphenol A differently inhibits CaV3.1, Ca V3.2 and Ca V3.3 calcium channels. *Naunyn Schmiedebergs Arch Pharmacol* **387**:153–163.

O'Reilly AO, Eberhardt E, Weidner C, Alzheimer C, Wallace BA, and Lampert A (2012) Bisphenol A binds to the local anesthetic receptor site to block the human cardiac sodium channel. *PLoS One* **7**:e41667.

Ogunbayo OA, Lai PF, Connolly TJ, and Michelangeli F (2008) Tetrabromobisphenol A (TBBPA), induces cell death in TM4 Sertoli cells by modulating Ca2+ transport proteins and causing dysregulation of Ca2+ homeostasis. *Toxicol In Vitro* **22**:943–952.

Ogunbayo OA and Michelangeli F (2007) The widely utilized brominated flame retardant tetrabromobisphenol A (TBBPA) is a potent inhibitor of the SERCA Ca2+ pump. *Biochem J* **408**:407–415.

Pandey AK and Deshpande SB (2012) Bisphenol A depresses compound action potential of frog sciatic nerve in vitro involving Ca(2+)-dependent mechanisms. *Neurosci Lett* **517**:128–132.

Periasamy M and Kalyanasundaram A (2007) SERCA pump isoforms: their role in calcium transport and disease. *Muscle Nerve* **35**:430–442.

Pessah IN, Cherednichenko G, and Lein PJ (2010) Minding the calcium store: ryanodine receptor activation as a convergent mechanism of PCB toxicity. *Pharmacol Ther* **125**:260–285.

Pessah IN, Stambuk RA, and Casida JE (1987) Ca2+-activated ryanodine binding: mechanisms of sensitivity and intensity modulation by Mg2+, caffeine, and adenine nucleotides. *Mol Pharmacol* **31**:232–238.

Posnack NG, Jaimes, IIIR, Asfour H, Swift LM, Wengrowski AM, Sarvazyan N, and Kay MW (2014) Bisphenol A exposure and cardiac electrical conduction in excised rat hearts. *Environ Health Perspect* **122**:384–390.

Rando TA and Blau HM (1994) Primary mouse myoblast purification, characterization, and transplantation for cell-mediated gene therapy. *J Cell Biol* **125**: 1275–1287.

Reistad T, Mariussen E, Ring A, and Fonnum F (2007) In vitro toxicity of tetrabromobisphenol-A on cerebellar granule cells: cell death, free radical formation, calcium influx and extracellular glutamate. *Toxicol Sci* **96**:268–278.

Rosenmai AK, Dybdahl M, Pedersen M, Alice van Vugt-Lussenburg BM, Wedebye EB, Taxvig C, and Vinggaard AM (2014) Are structural analogues to bisphenol a safe alternatives? *Toxicol Sci* **139**:35–47.

Salvatore D, Simonides WS, Dentice M, Zavacki AM, and Larsen PR (2014) Thyroid hormones and skeletal muscle–new insights and potential implications. *Nat Rev Endocrinol* **10**:206–214.

Shaw SD, Blum A, Weber R, Kannan K, Rich D, Lucas D, Koshland CP, Dobraca D, Hanson S, and Birnbaum LS (2010) Halogenated flame retardants: do the fire safety benefits justify the risks? *Rev Environ Health* **25**:261–305.

Soriano S, Ripoll C, Alonso-Magdalena P, Fuentes E, Quesada I, Nadal A, and Martinez-Pinna J (2016) Effects of bisphenol A on ion channels: experimental evidence and molecular mechanisms. *Steroids* **111**:12–20.

Sparks SE (2015) Neonatal hypotonia. *Clin Perinatol* **42**:363–371, ix ix.

Vandenberg LN, Chahoud I, Heindel JJ, Padmanabhan V, Paumgartten FJ, and Schoenfelder G (2010) Urinary, circulating, and tissue biomonitoring studies indicate widespread exposure to bisphenol A. *Environ Health Perspect* **118**: 1055–1070.

Vandenberg LN, Hauser R, Marcus M, Olea N, and Welshons WV (2007) Human exposure to bisphenol A (BPA). *Reprod Toxicol* **24**:139–177.

Vandenberg LN, Maffini MV, Sonnenschein C, Rubin BS, and Soto AM (2009) Bisphenol-A and the great divide: a review of controversies in the field of endocrine disruption. *Endocr Rev* **30**:75–95.

Verburg E, Dutka TL, and Lamb GD (2006) Long-lasting muscle fatigue: partial disruption of excitation-contraction coupling by elevated cytosolic Ca2+ concentration during contractions. *Am J Physiol Cell Physiol* **290**: C1199–C1208.

vom Saal FS, Akingbemi BT, Belcher SM, Birnbaum LS, Crain DA, Eriksen M, Farabollini F, Guillette, JrLJ, Hauser R, Heindel JJ, et al. (2007) Chapel Hill bisphenol A expert panel consensus statement: integration of mechanisms, effects in animals and potential to impact human health at current levels of exposure. *Reprod Toxicol* **24**:131–138.

Wang Q, Cao J, Zhu Q, Luan C, Chen X, Yi X, Ding H, Chen J, Cheng J, and Xiao H (2011) Inhibition of voltage-gated sodium channels by bisphenol A in mouse dorsal root ganglion neurons. *Brain Res* **1378**:1–8.

Wang W, Wang J, Wang Q, Wu W, Huan F, and Xiao H (2013) Bisphenol A modulates calcium currents and intracellular calcium concentration in rat dorsal root ganglion neurons. *J Membr Biol* **246**:391–397.

Westerink RH (2014) Modulation of cell viability, oxidative stress, calcium homeostasis, and voltage- and ligand-gated ion channels as common mechanisms of action of (mixtures of) non-dioxin-like polychlorinated biphenyls and polybrominated diphenyl ethers. *Environ Sci Pollut Res Int* **21**:6373–6383.

Woeste M, Steller J, Hofmann E, Kidd T, Patel R, Connolly K, Jayasinghe M, and Paula S (2013) Structural requirements for inhibitory effects of bisphenols on the activity of the sarco/endoplasmic reticulum calcium ATPase. *Bioorg Med Chem* **21**:3927–3933.

Yan S, Chen Y, Dong M, Song W, Belcher SM, and Wang HS (2011) Bisphenol A and 17β-estradiol promote arrhythmia in the female heart via alteration of calcium handling. *PLoS One* **6**:e25455.

Zamponi GW, Striessnig J, Koschak A, and Dolphin AC (2015) The physiology, pathology, and pharmacology of voltage-gated calcium channels and their future therapeutic potential. *Pharmacol Rev* **67**:821–870.

Zhou X, Guo J, Zhang W, Zhou P, Deng J, and Lin K (2014) Tetrabromobisphenol A contamination and emission in printed circuit board production and implications for human exposure. *J Hazard Mater* **273**:27–35.

Address correspondence to: Rui Zhang, Department of Molecular Biosciences, School of Veterinary Medicine, University of California, Davis, One Shields Avenue, Davis, CA 95616. E-mail: ruizhang@ucdavis.edu